ACS APPLIED MATERIALS & INTERFACES

Research Article

www.acsami.org

Membrane-Based Assay for Iodide Ions Based on Anti-Leaching of Gold Nanoparticles

Yu-Wei Shen,[†] Pang-Hung Hsu,[†] Binesh Unnikrishnan,[†] Yu-Jia Li,[†] and Chih-Ching Huang*[,†,‡,§]

[†]Institute of Bioscience and Biotechnology, National Taiwan Ocean University, 2 Beining Road, Keelung, 20224, Taiwan

[‡]Center of Excellence for the Oceans, National Taiwan Ocean University, Keelung, 20224, Taiwan

[§]School of Pharmacy, College of Pharmacy, Kaohsiung Medical University, Kaohsiung, 80708, Taiwan

Supporting Information

ABSTRACT: We report a label-free colorimetric strategy for the highly selective and sensitive detection of iodide (I^-) ions in human urine sample, seawater and edible salt. A poly(*N*-vinyl-2-pyrrolidone)-stabilized Au nanoparticle (34.2-nm) was prepared to detect I^- ions using silver (Ag^+) and cyanide (CN^-) ions as leaching agents in a glycine–NaOH (pH 9.0) solution. For the visual detection of the I^- ions by naked eye, and for long time stability of the probe, Au nanoparticles (NPs) decorated mixed cellulose ester membrane (MCEM) was prepared (Au NPs/MCEM). The Au NPs-based probe (CN^-/Ag^+–Au NPs/MCEM) operates on the principle that Ag^+ ions form a monolyar silver atoms/ions by aurophilic/argentophilic interactions on the Au NPs and it accelerates the leaching rate of Au atoms in presence of CN^- ions. However, when I^- is introduced into this system, it inhibits the leaching of Au atoms because of the strong interactions between Ag/Au ions and I^- ions. Inductively coupled plasma mass spectrometry, surface-assisted laser desorption/ionization time-of-flight mass spectrometry were used to characterize the surface properties of the Au NPs in the presence of Ag^+ and I^-. Under optimal solution conditions, the CN^-/Ag^+–Au NPs/MCEM probe enabled the detection of I^- by the naked eye at nanomolar concentrations with high selectivity (at least 1000-fold over other anions). In addition, this cost-effective probe allowed the determination of I^- ions in complex samples, such as urine, seawater, and edible salt samples.

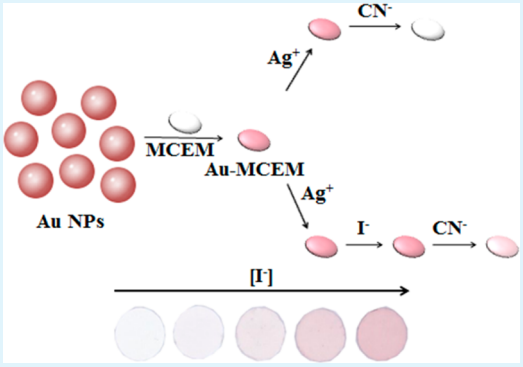

KEYWORDS: *gold nanoparticles, cellulose membranes, colorimetry, cyanide, leaching, iodide*

INTRODUCTION

The amount of iodine in the body is closely related to the health of the thyroid gland because iodine is necessary for the synthesis of thyroid hormones.[1−3] Inadequate intake of iodine causes hypothyroidism, cretinism, miscarriages, and mental retardation, while excessive intake leads to Jod–Basedow effect.[4−8] Therefore, the World Health Organization recommends an iodine intake of 150 μg per day for people above age twelve.[9] Iodine and iodide (I^-) are both present in the environment; the iodine content is approximately 50–80 ppb in seawater and 1–20 ppm in soil.[10−13] The iodine present in the environment is passed through the food chain to both marine and terrestrial flora and fauna; therefore, most of the marine and terrestrial flora and fauna contain trace amounts of iodine.[14−19] However, iodine intake by humans is mostly through their diet, and trace amounts from drinking water.[20−22] Although seawater contains iodine, sea salt contains only 1.4 ppm iodine that is available to humans. Because an adult requires only 6 g of salt each day, iodine intake from sea salt may not be sufficient.[23−25] Therefore, to increase the intake of iodine many commercial edible salts contain potassium iodate. Any excess iodine consumed by humans is excreted through urine in the form of iodide ions (I^-),[26−28] because the organs in the human body cannot store iodine. Thus, detection of I^- ions in environmental, food, and biological samples, such as water, edible salts, and urine is important.

The detection of iodine in high salt containing samples such as seawater, edible salt and biological sample such as urine is a challenge. Various methods have been developed for the determination of the I^- concentration in real samples.[26−49] Inductively coupled plasma mass spectrometry (ICP-MS) can detect iodide with good sensitivity, but requires the use of an internal standard.[29−31] Zheng et al. used multimode size-exclusion chromatography with sector-field ICP-MS to reduce the matrix effect for iodine detection in seawater.[29] Inductively coupled plasma atomic emission spectrometry can efficiently detect iodine in real samples (milk powder and iodized salt).[32−34] Similarly, gas chromatography–mass spectrometry,[35−37] anion-exchange/reversed-phase high performance liquid chromatography,[38−40] chromogenic and fluorogenic chemosensors were recently developed for the detection of I^-.[41−46] Although the above-mentioned methods can detect

Received: November 9, 2013
Accepted: January 9, 2014
Published: January 9, 2014

   dx.doi.org/10.1021/am405027q | ACS Appl. Mater. Interfaces 2014, 6, 2576−2582

iodine or iodide, they still have some drawbacks, such as complex sample preparation, biological sample's matrix interference, professional instrument operation, and expensive equipment.

In recent years, many types of nanoparticle (NP)-based techniques have been developed to detect iodine and iodide, including spectrophotometry (absorption, fluorescence, and Raman), mass spectrometry, and electrochemistry methods.[47−59] I^--induced fluorescence quenching of the Ag NCs and I^--induced shape change of irregularly shaped core/shell Cu@AuNPs to regular shaped NPs have been employed for iodide determination.[47,50] Silver nanowire-modified electrodes have been used efficiently detect I^- ions by electrochemical techniques.[56] Recently, we reported the detection of I^- ions by monitoring gold−iodide hybrid cluster ions generated from Au NPs-modified cellulose membrane under pulsed laser irradiation using mass spectrometry, up to concentrations as low as 0.5 nM.[59] Because of the unique optical and electrochemical properties of NPs, these NPs-based sensors exhibit high sensitivity for the detection of I^- in aqueous solutions. However, these NP-based sensors also suffer from some limitations, such as the poor stability of the NPs, complex detection procedures, matrix interference, interference of metal ions and other anions, and high cost. In addition to the aforementioned shortcomings, these NP-based sensors are rarely applied for complicated sample testing.

Therefore, in this study, we developed a colorimetric method to sense I^- in aqueous media based on the antileaching of Au NPs by I^- ions. Reaction of Au NPs with silver ions (Ag^+) in solution led to the self-deposition of the Ag^+ ions on the surfaces of the Au NPs. After addition of CN^- to the solution, very rapid leaching of Au NPs resulted in a large decrease in the surface plasmon resonance (SPR) absorption band for the Au NP solution. However, addition of I^- prior to CN^- led to retardation of the Ag^+-accelerated leaching rate of the Au NPs induced by CN^- (Scheme 1A). Moreover, fabrication of an Au NPs-modified membrane by simple adsorption of Au NPs onto a mixed cellulose ester membrane (MCEM) provided a simple paper-based colorimetric sensor for the rapid detection of I^- ions (Scheme 1B). Notably, the Au NPs/MCEM enabled the detection of I^- by the naked eye in the nanomolar range in aqueous solutions in the presence of Ag^+ and CN^-.

Scheme 1. Illustration of the Sensing Mechanism of the (A) CN^-/Ag^+−Au NPs Probe and (B) CN^-/Ag^+−Au NPs/MCEM for the Detection of I^- Ions

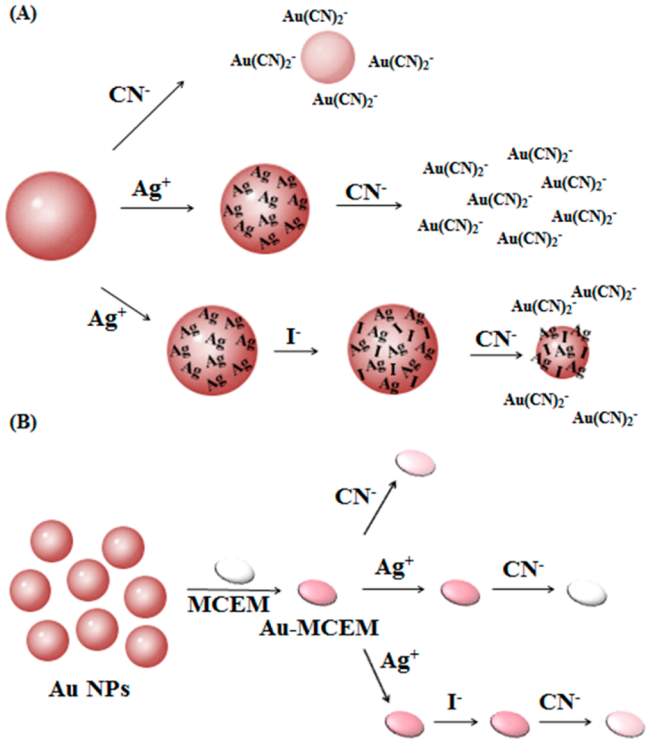

MATERIALS AND METHODS

Chemicals. Trisodium citrate, phosphoric acid, and citric acid monohydrate were purchased from Sigma-Aldrich (St. Louis, MO). MCEM (pore size = 0.45 μm; thickness = 145 μm; porosity ≈ 75%) was purchased from Advantec (Toyo Roshi Kaisha, Japan). Hydrogen tetrachloroaurate (III) trihydrate ($HAuCl_4{\cdot}3H_2O$), trisodium citrate, silver nitrate ($AgNO_3$), and hydrogen peroxide (H_2O_2) were obtained from Acros (Geel, Belgium). NaCN, NaSCN, CH_3COONa, NaBr, NaCl, $NaClO_4$, KI, $NaNO_3$, Na_3PO_4, Na_2S, $Na_2S_2O_3$, Na_2SO_4, KIO_3, $Na_2AsO_4{\cdot}7H_2O$, and H_2O_2 were obtained from Alfa Aesar (Ward Hill, MA). The buffer was a 50 mM glycine solution (pH 9.0, adjusted with 1.0 N NaOH). Poly(*N*-vinyl-2-pyrrolidone) (PVP; M_w = 360 000) and all other unspecified reagents used in this study were purchased from Sigma-Aldrich. Milli-Q ultrapure water (Millipore, Billerica, MA) was used in all of the experiments.

Preparation of Au NPs and Fabrication of the Au NPs/MCEM. The Au NPs (34.2-nm) were synthesized as previously reported.[60] Briefly, a 1% trisodium citrate solution (0.5 mL) was rapidly added to $HAuCl_4$ solution (0.01%, 50 mL) in a flask equipped with a reflux condenser and boiled for 8 min. The dimensions of the Au NPs were measured using a transmission electron microscope (TEM, H7100, Hitachi High-Technologies Corporation, Tokyo, Japan); Au NPs appeared to be nearly monodisperse, with an average size of 34.2 ± 3.6 nm (from 100 counts). The concentration of the 34.2-nm Au NPs was 0.28 nM assuming ideal spherical particles and using eq 1

$$n = 3m/4\pi r^3 s \quad (1)$$

where n is the number of Au particles per milliliter, m is the concentration (g mL^{-1}) of Au in the substance, r is the particle radius (cm), and s is the specific gravity of colloidal Au (19.3 g cm^{-3}). The values of m and r were determined from the results of ICP-MS and TEM analysis, respectively. The concentration obtained from the results was then converted into the number of Au particles per liter and divided by Avogadro's number to obtain the final molar concentration of Au NPs. The synthesized Au NPs were then coated with PVP (0.02%) in 10 mM glycine−NaOH (pH 9.0). The as-prepared PVP-coated Au NPs remained stable in solutions containing up to 500 mM NaCl (Figure S1, Supporting Information).

An MCEM with a diameter of 0.6 cm was used for the preparation of the Au NPs/MCEM substrate. The MCEM was immersed in Au NPs (140 pM)-containing citrate solution (20 mL, 3 mM, pH 5.0) and incubated for 2 h. The Au NPs-adsorbed MCEM (Au NPs/MCEM) was then gently washed with ultrapure water (20 mL) and dried in air for 2 h at room temperature.

Detection of I^- Ions Using the Au NPs-Based Probe. For the sensing of I^- ions, aliquots of (250 μL) of glycine-NaOH (pH 9.0) solution containing the Au NPs were equilibrated with 50 μL of Ag^+ solution for 10 min. Then, 50 μL of PVP solution was added as a stabilizer and mixed well. After 10 min, 50 μL of different concentrations of I^- solutions/samples were added and kept undisturbed for 30 min. Then, 50 μL of NaCN solution was added, mixed well and kept for 2 h at room temperature. The mixtures were then transferred separately into 96-well microtiter plates, where their UV−vis absorption spectra were recorded using a μQuant monochromatic microplate spectrophotometer (Biotek Instruments, Winooski, VT, USA). In this article, the final concentrations of the species are provided.

dx.doi.org/10.1021/am405027q | ACS Appl. Mater. Interfaces 2014, 6, 2576−2582

Detection of I^- Ions Using the Membrane-Based Probe. To sense I^- ions, the as-prepared Au NPs/MCEM was immersed in (700 μL) of glycine–NaOH (pH 9.0) solution containing the Ag^+ for 10 min. Then, the PVP solution (100 μL) was added into the Au NPs/MCEM containing solution and kept for 10 min. The different concentrations of KI solution/samples (100 μL) were then added to it and incubated for 30 min. Subsequently, NaCN was added and reacted for another 2 h. The membranes were then gently washed with DI water (~20 mL) and dried with an air blow gun (60 Lb/in^2) for 1 min prior to analysis. To perform the color analysis, the prepared membrane was scanned using an Epson desktop scanner (Epson Perfection 1660 Photo Scanner), and the color intensity of the pixels (red, green, and blue) was analyzed using the Image J computer program (National Institutes of Health, USA). The green absorption component (G_{abs}) of the image of the Au NPs/MCEM was used to quantify the Au NPs. The value of G_{abs} (8-bit, with brightness values from 0 to 255) is related to the quantitation of the Au NPs. A high value of G_{abs} indicates a decrease in the intensity of the observed red color, and thus a high amount of leaching of the Au NPs.

Analysis of I^- in Real Samples. Three edible salt samples containing different concentrations of KIO_3 were purchased from Taiwan Salt Industrial Corporation (Miaoli, Taiwan). For the analyses, a 0.02 g/mL solution of each edible salt was prepared in ultrapure water and then treated with 5.0 mM ascorbic acid for 10 min to reduce IO_3^- to I^-. Aliquots of these solutions (1.0 mL) were then diluted 200-fold with 10 mM glycine–NaOH (pH 9.0). The samples were then separately analyzed using ICP-MS and the Ag^+/CN^-–Au NPs/MCEM probe. Urine samples collected from five healthy humans (20–30 years old) in the early morning were used for testing iodide content in it, because metabolite levels in urine may vary during the day. The insoluble materials in the urine samples were removed by centrifugation (RCF 3000 g, 30 min) and filtered through a 0.2 μm membrane. The filtered urine was then diluted 50-fold with 10 mM glycine–NaOH (pH 9.0) containing 100 mM H_2O_2 and divided into 1.0 mL aliquots. Each sample was separately analyzed using ICP-MS and Ag^+/CN^-–Au NPs/MCEM probe. A sample of seawater from the East China Sea was filtered through a 0.2 μm membrane and analyzed using ICP-MS. Aliquots of the seawater (25 μL) were then spiked with standard I^- solutions (100 μL) to achieve final concentrations in the range from 0 to 75 nM. The mixtures were diluted to 1.0 mL with 10 mM glycine–NaOH (pH 9.0) containing Ag^+ (400 nM) and then analyzed using the present approach with the Au NPs/MCEM probe.

RESULTS AND DISCUSSION

Antileaching-Based Sensor for I^- Ions. Scheme 1A depicts the label-free Au NPs probe that was used for the detection of I^- ions. Curve A in Figure 1 displays the absorption spectrum of PVP-stabilized Au NPs (70 pM; average diameter = 34.2 ± 3.6 nm from 100 counts) in a 10 mM glycine–NaOH solution (pH 9.0); a strong SPR absorption appears at 526 nm (extinction coefficient ~1.2 × 10^9 M^{-1} cm^{-1}). When the 34.2-nm Au NPs (70 pM) were reacted with Ag^+ (400 nM) in a 10 mM glycine–NaOH (pH 9.0) solution, a Ag–Au alloy was formed immediately on the surfaces of the Au NPs via strong aurophilic/argentophilic bonding and a slight galvanic replacement reaction.[61−67] As a result, the SPR absorption band of the Au NPs at 526 nm increased slightly (curve B in Figure 1). Since the Au NPs were equilibrated with the Ag^+ ions and then stabilized with PVP before adding I^- solution, PVP prevented the aggregation of particles in the presence of I^- ions. The steric repulsive force between the PVP-modified Au NPs is the main contributor toward the dispersion of particles in the solution. Stabilization of Au NPs by polymers is much less sensitive toward changes in the ionic strength of the solution than that of use of small ionic compounds. There was no statistical difference in the average particle diameter or size distribution of the Au NPs in the absence and presence of 400 nM Ag^+ ions as determined from TEM images (Figure S2A and S2B, Supporting Information), revealing that there was only a monolayer or submonolayer of Ag on the surfaces of the Au NPs. Also, we conducted the dynamic light scattering experiment (DLS) to observe any change in the hydrodynamic diameter of Au NPs in the absence and presence of Ag^+ (400 nM) (Figure S3, Supporting Information). It shows that the Au NPs and Ag^+-Au NPs have almost same particle size distributions. Next, ICP-MS was used to quantify the content of Ag species on the Au NPs, and it was determined that >98% of the Ag^+ atoms/ions were bonded to Au NPs (~6000 Ag atoms/ions per Au NP). To test the interaction of Ag^+ with PVP in our experimental conditions, silver nitrate solution (400 nM) was mixed with 0.02% PVP solution (same as that of experimental conditions) and UV–vis absorption spectra was recorded. We did not observe any characteristic plasmon peaks corresponding to the formation of Ag nanoparticles because of the reduction of Ag^+ by PVP in the duration of our experiment (Figure S4, Supporting Information). This may be due to the low concentrations of the reagents, low temperature and very low reaction time. Therefore, the reduction of Ag^+ to Ag can be ruled out. PVP contains oxygen and nitrogen groups that interact with Ag/Ag^+ and give stability to the system.

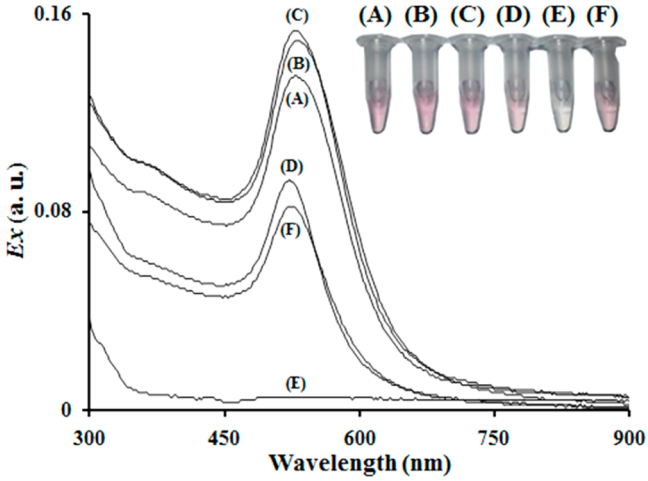

Figure 1. UV–vis absorption spectra of solutions of (A) Au NPs (70 pM); (B) Au NPs (70 pM) and Ag^+ (400 nM); (C) Au NPs (70 pM), Ag^+ (400 nM), and I^- (1 μM); (D) Au NPs (70 pM) and CN^- (150 μM); (E) Au NPs (70 pM), Ag^+ (400 nM), and CN^- (150 μM); and (F) Au NPs (70 pM), Ag^+ (400 nM), I^- (1 μM), and CN^- (150 μM). All of the solutions were prepared in a 10 mM glycine–NaOH solution (pH 9.0). The inset: photographic images of the Au NPs solutions. The extinction (Ex) values are plotted in arbitrary units (a.u.).

Notably, the dissolved oxygen gas (O_2) in the NaCN-leaching liquor that was added to the Au NPs acted as an oxidant [$4Au + 8CN^- + O_2 + 2H_2O \rightarrow 4Au(CN)_2^- + 4OH^-$; stability constant for $Au(CN)_2^-$ ~10^{39}].[68−70] The average size of the Au NPs decreased from 34.2 ± 3.6 nm to 26.3 ± 5.4 nm after reaction with CN^- for 2 h in the absence of Ag^+ (Supporting Information Figure S2D). As a result, the SPR absorption of the Au NPs at 526 nm decreased dramatically (curve D in Figure 1). However, in the presence of 400 nM Ag^+, the Ag^+ induced nearly complete leaching of the Au NPs by the leaching agent (150 μM CN^-) as revealed in the UV–vis absorption spectrum (curve E in Figure 1) and TEM images (Supporting Information Figure S2E) of the Au NPs. The

deposition of Ag atoms/ions on the Au NPs created a relatively unstable lattice structure on the surfaces of the particles, and therefore accelerated the dissolution of the Au NPs and the formation of $Au(CN)_2^-$ in solution. As a result, the SPR absorption band of the Au NPs at 526 nm nearly disappeared. On the other hand, the particle size of the Au NPs only slightly decreased from 34.2 ± 3.6 to 24.6 ± 6.2 nm in the presence of I^- (1 μM), Ag^+ (400 nM), and CN^- (150 μM), indicating that the I^- strongly retarded the leaching rate of the Au NPs. This result suggests that the strong interactions between Ag–I [$K_{sp}(AgI) = 8.3 \times 10^{-17}$; $K_f(AgI_2^-) = 1.0 \times 10^{11}$] and Au–I [$K_f(AuI_2^-) = 7.9 \times 10^{18}$] on the surfaces of the particles inhibit the access of CN^- to the surfaces of the Au NPs.[71−73] Notably, using surface-assisted laser desorption/ionization time-of-flight mass spectrometry (LDI-MS), signals were observed for $[AgI]^-$, $[AuI]^-$, $[AgI_2]^-$, $[AuI_2]^-$, and $[Au_2I]^-$ at m/z values of 233.81, 323.87, 360.71, 450.78, and 520.84, respectively, which confirmed the formation of stable Ag–I and Au–I complexes on the surfaces of the Au NPs (Figure S5, Supporting Information).

Effect of the CN^- and Ag^+ Concentrations. The effects of the CN^- (0–400 μM) and Ag^+ (0–750 nM) concentrations on the leaching of Au NPs in the absence and presence (100 nM) of I^- ions was then investigated. The rate of dissolution of Au NPs in the solution increased as the CN^- concentration increased (Figure 2A). Moreover, at a constant CN^- concentration, the rate of dissolution of Au NPs in the solution increased with an increase in the concentration of Ag^+ in the absence of I^- ions. In addition, the rate of leaching decreased in the presence of I^- ions (100 nM) at constant concentrations of CN^- (within the range 50–400 μM) and Ag^+ (within the range 50–750 nM) (Figure 2B). The maximum value of $(Ex_{526} - Ex^0_{526})/Ex^0_{526}$ for the Au NPs in the presence and absence of I^- (100 nM) was observed at 150 μM CN^- and 400 nM Ag^+, respectively (Figure 2C). Here Ex^0_{526} and Ex_{526} are the extinction values for the CN^-/Ag^+–Au NPs probe in the absence and presence of I^- (100 nM), respectively.

Sensitivity and Selectivity. Using solutions of Au NPs (70 pM) in the presence of CN^- (150 μM)/Ag^+ (400 nM), a linear relationship (r = 0.98) between the values of $(Ex_{526}–Ex^0_{526})/Ex^0_{526}$ for the Au NPs and the concentration of I^- ions was obtained in the range from 0.05 to 1.00 μM (Figure S6, Supporting Information). The limit of detection (S/N ratio = 3) for the I^- ions was 25 nM. To evaluate the selectivity of the proposed colorimetric assay, we then determined the values for $(Ex_{526} - Ex^0_{526})/Ex^0_{526}$ for the CN^-/Ag^+–Au NPs probe in the presence of different anions (100 nM for I^- and 10 μM for each other anion). It was found that I^-, S^{2-}, $S_2O_3^{2-}$, and AsO_4^{3-} strongly retarded the leaching of the Au NPs, while the other tested anions had an insignificant effect under the same experimental conditions (Figure S7, Supporting Information). It is possible that the formation of highly stable Ag_2S [$K_{sp} \approx 6 \times 10^{-51}$] and Au_2S ($K_{sp} \approx 3 \times 10^{-55}$) on the surfaces of the Au NPs may be the main reason for the decrease in the leaching rate of the Au NPs. In addition, the reaction of between CN^- and AsO_4^{3-} ($AsO_4^{3-} + CN^- + H_2O \rightarrow AsO_2^- + CNO^- + 2OH^-$) resulted in the lower leaching rate in the presence of AsO_4^{3-}. Moreover, $S_2O_3^{2-}$ is a divalent-type soft ligand that tends to form stable complexes with low-spin d^{10} Au^+ ions and Ag^+ ($K_f \approx 10^{26}$) on the surfaces of particles,[74] and thus CN^--induced leaching was reduced. H_2O_2 possesses a strong oxidizing ability ($E^0 = -0.695$ V) for S^{2-} ($S^{2-} + 4H_2O_2 \rightarrow SO_4^{2-} + 4H_2O$) and $S_2O_3^{2-}$ ($2S_2O_3^{2-} + H_2O_2 \rightarrow S_4O_6^{2-} +$

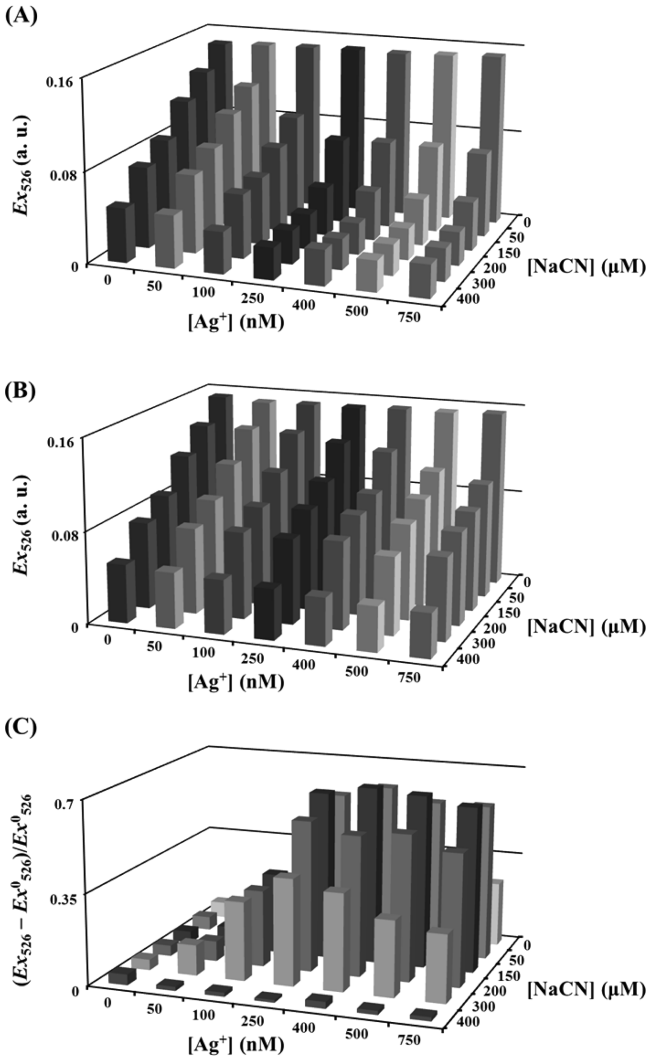

Figure 2. Ex_{526} values for CN^-/Ag^+–Au NP (70 pM) solutions in the (A) absence and (B) presence of I^- (100 nM). (C) $(Ex_{526}–Ex^0_{526})/Ex^0_{526}$ values for the Au NPs in a 10 mM glycine–NaOH solution (pH 9.0) containing Ag^+ (0–750 nM) and CN^- (0–400 μM) for sensing of I^- (100 nM). Conditions were otherwise the same as those described in Figure 1

$2OH^-$) and accelerating the leaching of Au NPs under alkaline conditions.[75,76] Therefore, the use of H_2O_2 (100 mM) as masking agent and/or oxidation agent (assistant leaching agent) greatly suppressed the interference from S^{2-}, $S_2O_3^{2-}$, and AsO_4^{3-} anions, allowing the CN^-/Ag^+–Au NPs sensor to exhibit excellent selectivity toward I^- (Supporting Information Figure S7). H_2O_2 oxidizes I^- ions only in highly acidic medium. Since we conducted the detection of I^- in alkaline medium, the possibility of this reaction can be ruled out. The selectivity studies (Supporting Information Figure S7) suggest that H_2O_2 efficiently eliminated the interference due to the S^{2-}, $S_2O_3^{2-}$, and AsO_4^{3-} ions during the determination of I^- ions. The CN^-/Ag^+–Au NPs (70 pM) in 10 mM glycine–NaOH buffer (pH 9.0) containing H_2O_2 (100 mM) thus exhibited a 1000-fold selectivity for I^- over other anions.

Cellulose Membrane-Based Sensor for I^-. Next, the Au NPs/MCEM was used as a simple, membrane-based Au NPs probe for the visual detection of I^- in real, environmental, biological, and edible salt samples. The scanning electron microscopy (SEM) image (Figure S8A, Supporting Informa-

dx.doi.org/10.1021/am405027q | ACS Appl. Mater. Interfaces 2014, 6, 2576–2582

tion) and UV−vis absorption spectra (Figure S9, Supporting Information) of the Au NPs/MCEM confirmed that the Au NPs adsorbed on the MCEM surfaces did not form aggregates. Analysis of the color and LDI-MS image of the Au NPs/MCEM (Figure S10, Supporting Information) further confirmed that the cellulose fibers associated homogenously with the adsorbed Au NPs. Notably, the CN^-/Ag^+−Au NPs/MCEM probe enabled the detection of I^- at concentrations as low as 2 nM in 10 mM glycine−NaOH (pH 9.0) (Figure 3).

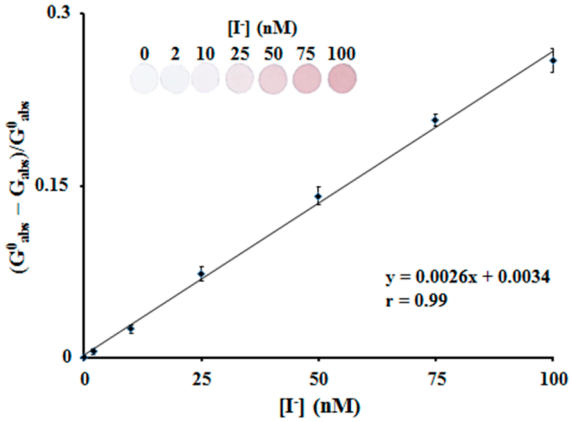

Figure 3. Validation of the use of the CN^-/Ag^+−Au NPs/MCEM in the presence of H_2O_2 (100 mM) for sensing I^- ions (0−100 nM) in 10 mM glycine−NaOH (pH 9.0). Error bars are standard deviation values across four repetitive experiments. Conditions otherwise were the same as those described in Figure 1.

Moreover, the detection sensitivity of the CN^-/Ag^+−Au NPs/MCEM membrane sensor is increased up to 10-fold over the free Au NPs because of the ability of I^- ions to deposit on the Au NPs/MCEM, even from a very dilute aqueous solution.

Analysis of I^- in Real Samples and Probe Stability. To validate the proposed sensing strategy and confirm its practical application for I^- analysis in environmental samples, the CN^-/Ag^+−Au NPs/MCEM sensor was used to determine the levels of I^- in highly saline seawater samples (Figure 4). Applying standard addition methods to our new approach and ICP-MS-based analysis, the concentration of I^- ions in the seawater sample was determined to be 0.35 ± 0.04 μM (n = 4) and 0.31 ± 0.02 μM (n = 4), respectively. The Student's t-test and F-test values for the correlation between the two methods were 1.77 and 4.00, respectively (the t-test and F-test values were 2.45 and 9.28, respectively, at 95% confidence), suggesting that the two methods did not provide significantly different results. The CN^-/Ag^+−Au NPs/MCEM was then used for the analysis of I^- ions in complicated human urine samples. Figure 5A displays the color of the Au NPs/MCEMs after reacting with 50-fold diluted urine collected from five healthy humans (20−30 years old) in the presence of CN^- (150 μM), Ag^+ (400 nM), and H_2O_2 (100 mM) in 10 mM glycine−NaOH (pH 9.0) buffer. Figure 5B reveals the good linear correlation (r = 0.97) between the results obtained for $[(G^0_{abs}-G_{abs})/G^0_{abs}]$ (G^0_{abs} and G_{abs} are the green component absorbance of the Au NPs/MCEM after reacting with the leaching agents in the absence and presence of 50-fold diluted urine samples, respectively) using the membrane-based assay and ICP-MS over concentrations ranging from 0.12 to 1.61 μM, indicating that the proposed probe can be applied for the determination of I^- ions in urine. Finally, the membrane-based sensing strategy was also

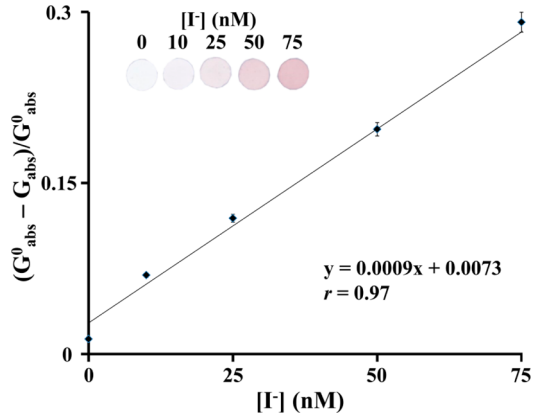

Figure 4. Analyses of the I^- concentration in seawater samples using the CN^-/Ag^+−Au NPs/MCEM probes. The pretreated seawater samples were spiked with I^- ions at concentrations ranging from 0 to 75 nM and then analyzed using the CN^-/Ag^+−Au NPs/MCEM probes. G^0_{abs} and G_{abs} are the green component absorbance of the Au NPs/MCEM in the absence and presence of I^--spiked seawater samples (40-fold dilution), respectively. Conditions otherwise were the same as those described in Figure 3

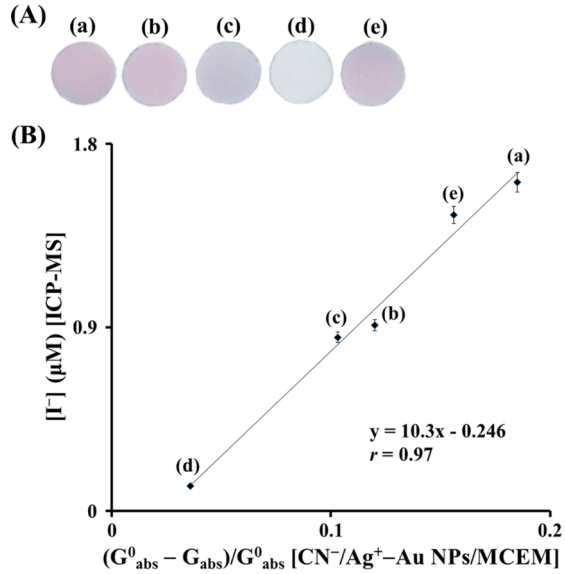

Figure 5. (A) Photographic images recorded using the Au NPs/MCEM for the detection of I^- in five (a−e) human urine samples (50-fold dilution). (B) Comparison of the CN^-/Ag^+−Au NPs/MCEM probe and the ICP-MS results for the determination of I^- in five human urine samples (a−e).

used to determine the iodine content in three different edible salt samples. The I^- concentrations in one of the representative edible salts were first determined using the estimated standard addition method (Figure S11, Supporting Information). Table 1 shows the t-test data for a comparison of the results obtained for the I^- concentration using the CN^-/Ag^+−Au NPs/MCEM system with the certified values for each sample at a 95% confidence interval, and it can be clearly seen that the results are in good agreement. Furthermore, the membrane-based probe was used to easily screen the iodine levels in the edible salt samples with the naked eye (Figure S12, Supporting Information). A comparison of the sensing parameters of other colorimetric/fluorometric iodide sensors is given in Table S1 (Supporting Information). The LOD of our probe for I^- ions is

dx.doi.org/10.1021/am405027q | ACS Appl. Mater. Interfaces 2014, 6, 2576−2582

Table 1. Determination of I^- Concentrations in Edible Salt Samples Using the CN^-/Ag^+−Au NPs/MCEM Probe and ICP-MS

salt sample	certified range (ppm)	ICP-MS, mean ± SD (ppm, n = 5)	Au NPs/MCEM, mean ± SD (ppm, n = 5)	t-test between ICP-MS and Au NPs/MCEM[a]	consensus value (ppm), 95% confidence interval[a]
sample A	0	ND[b]	ND[b]		
sample B	15.2	15.6 ± 2.6	16.7 ± 2.2	1.69	15.9−17.5
sample C	15.0−35.5	27.9 ± 4.2	28.9 ± 3.5	1.63	28.0−29.8

[a]t-test value is 2.31 at a 95% confidence level (degree of freedom = 8). [b]Not detected.

comparable or better than those obtained using other nanomaterial-based optical sensors. Notably, most reported NPs-based sensors are rarely applied for the determination of I^- ion concentrations in complex environmental and biological samples, because NPs readily aggregate in highly saline solutions and often there is significant interference from background proteins and aminothiols.[47−55] Thus, although the new label-free assay is less sensitive than ICP-MS analysis, it is relatively simple and cost-effective. In addition, with the CN^-/Ag^+−Au NPs/MCEM probe, it is easy to detect I^- concentrations below 2 nM using the naked eye. We further studied the stability of the detection probe (both Au NPs and Au NPs/MCEM). The Au NPs solution was stable for at least 3 months when stored at 4 °C in the dark (Figure S13 in the Supporting Information), while, the Au NPs/MCEM after 9 months of preparation showed only 0.59% decrease in the G_{abs} value as that of the freshly prepared Au NPs/MCEM, indicating the high storage stability of the probes (Figure S14 in the Supporting Information).

CONCLUSIONS

We demonstrated that the rate of leaching of Au NPs by CN^- in aqueous solution can be increased in the presence of Ag^+ ions and decreased by I^- ions because of the formation of Ag−I and Au−I complexes on the surfaces of the Au NPs. The antileaching property can be effectively used for I^- determination in urine, seawater, and edible salt samples. Furthermore, the use of H_2O_2 as masking agent and/or oxidant eliminated the interference from S^{2-}, $S_2O_3^{2-}$, and AsO_4^{3-} and showed excellent specificity for I^- detection. Additionally, a CN^-/Ag^+−Au NPs/MCEM probe allowed selective detection of I^- at concentrations as low as 2 nM using the naked eye. Therefore, in comparison to other NPs-based optical methods,[47−55] the CN^-/Ag^+−Au NPs/MCEM probe for the detection of I^- is relatively simple, selective, sensitive, and cost-effective. Notably, NP-based probes tend to suffer from matrix interference in the presence of the high concentrations of salts, proteins, and amino thiols that are typically present in real biological and environmental samples. Thus, NPs-based probes are rarely applied for the determination of I^- in real samples (particularly seawater and urine), but the new, simple, label-free colorimetric sensor can be used for the detection of I^- during field operations. The practical application of the probe was validated with the analysis of I^- in urine, seawater, and edible salt samples and also the storage stability.

ASSOCIATED CONTENT

Supporting Information

TEM, LDI-MS, UV−vis absorption spectra, selectivity experiment, SEM, color analysis of membrane, salt sample analysis, photographic images of membranes, and comparison of sensing parameters. This information is available free of charge via the Internet at http://pubs.acs.org.

AUTHOR INFORMATION

Corresponding Author

*Tel.: 011-886-2-2462-2192, ext: 5517. Fax: 011-886-2-2462-2034. E-mail: huanging@ntou.edu.tw.

Notes

The authors declare no competing financial interest.

ACKNOWLEDGMENTS

This study was supported by the National Science Council of Taiwan under contract NSC 101-2628-M-019-001-MY3, 102-2113-M-019-001-MY3 and 102-2627-M-019-001-MY3.

REFERENCES

(1) Basalaeva, N. L. *Biol. Trace Elem. Res.* **2013**, *154*, 244−254.
(2) Krassas, G. E.; Poppe, K.; Glinoer, D. *Endocr. Rev.* **2010**, *31*, 702−755.
(3) Hess, S. Y. *Best Pract. Res. Clin. Endocrinol. Metab.* **2010**, *24*, 117−132.
(4) Hetzel, B. S. *Lancet* **1983**, *322*, 1126−1129.
(5) Dillon, J. C.; Milliez, J. *Br. J. Obstet. Gynaecol.* **2000**, *107*, 631−636.
(6) Delange, F. *Postgrad. Med. J.* **2001**, *77*, 217−220.
(7) Delange, F. *Proc. Nutr. Soc.* **2000**, *59*, 75−79.
(8) Lee, K.; Bradley, R.; Dwyer, J.; Lee, S. L. *Nutr. Rev.* **1999**, *57*, 177−181.
(9) de Benoist, B.; Andersson, M.; Egli, I.; Takkouche, B.; Allen, H. *WHO Global Database on Iodine Deficiency*; World Health Organization: Geneva, 2004.
(10) Truesdale, V. W. *Deep-Sea Res.* **1974**, *21*, 761−766.
(11) Truesdale, V. W. *Mar. Chem.* **1978**, *6*, 253−273.
(12) Muramatsu, Y.; Wedepohl, K. H. *Chem. Geol.* **1998**, *147*, 201−216.
(13) Mani, D.; Kumar, T. S.; Rasheed, M. A.; Patil, D. J.; Dayal, A. M.; Rao, T. G.; Balaram, V. *Nat. Resour. Res.* **2011**, *20*, 75−88.
(14) Fuge, R.; Johnson, C. C. *Environ. Geochem. Health* **1986**, *8*, 31−54.
(15) Korobova, E. *J. Geochem. Explor.* **2010**, *107*, 180−192.
(16) Tensho, K.; Yeh, K.-L. *Soil. Sci. Plant Nutr.* **1970**, *16*, 30−37.
(17) Haldimann, M.; Alt, A.; Blanc, A.; Blondeau, K. *J. Food Compos. Anal.* **2005**, *18*, 461−471.
(18) Eckhoff, K. M.; Maage, A. *J. Food Compos. Anal.* **1997**, *10*, 270−282.
(19) Dierick, N.; Ovyn, A.; de Smet, S. *J. Sci. Food Agric.* **2009**, *89*, 584−594.
(20) Anke, M.; Groppel, B.; Müller, M.; Scholz, E.; Krämer, K. *Fresen. J. Anal. Chem.* **1995**, *352*, 97−101.
(21) Pedersen, K. M.; Laurberg, P.; Nøhr, S.; Jørgensen, A.; Andersen, S. *Eur. J. Endocrinol.* **1999**, *140*, 400−403.
(22) Lee, S. M.; Lewis, J.; Buss, D. H.; Holcombe, G. D.; Lawrance, P. R. *Br. J. Nutr.* **1994**, *72*, 435−446.
(23) He, F. J.; MacGregor, G. A. *Hypertension* **2003**, *42*, 1093−1099.
(24) He, F. J.; MacGregor, G. A. *Prog. Cardiovasc. Dis.* **2010**, *52*, 363−382.
(25) Zimmermann, M. B.; Zeder, C.; Chaouki, N.; Saad, A.; Torresani, T.; Hurrell, R. F. *Am. J. Clin. Nutr.* **2003**, *77*, 425−432.
(26) Macours, P.; Aubry, J. C.; Hauquier, B.; Boeynaems, J. M.; Goldman, S.; Moreno-Reyes, R. *J. Trace Elem. Med. Biol.* **2008**, *22*, 162−165.

(27) Moussa, F.; Raux-Demay, M.-C.; Veinberg, F.; Depasse, F.; Gharbi, R.; Hautem, J.-Y.; Aymard, P. *J. Chromatogr., B: Anal. Technol. Biomed. Life Sci.* **1995**, *667*, 69−74.
(28) Valentín-Blasini, L.; Blount, B. C.; Delinsky, A. *J. Chromatogr. A* **2007**, *1155*, 40−46.
(29) Zheng, J.; Yamada, M.; Yoshida, S. *J. Anal. At. Spectrom.* **2011**, *26*, 1790−1795.
(30) Chen, Z.; Megharaj, M.; Naidu, R. *Talanta* **2007**, *72*, 1842−1846.
(31) Liao, H.; Zheng, J.; Wu, F.; Yamada, M.; Tan, M.; Chen, J. *Appl. Radiat. Isot.* **2008**, *66*, 1138−1145.
(32) Matusiewicz, H.; Ślachciński, M. *Anal. Methods* **2010**, *2*, 1592−1598.
(33) Niedobová, E.; Machát, J.; Otruba, V.; Kanický, V. *J. Anal. At. Spectrom.* **2005**, *20*, 945−949.
(34) Naozuka, J.; da Veiga, M. A. M. S.; Oliveira, P. V.; de Oliveira, E. *J. Anal. At. Spectrom.* **2003**, *18*, 917−921.
(35) Zhang, S.; Schwehr, K. A.; Ho, Y.-F.; Xu, C.; Roberts, K. A.; Kaplan, D. I.; Brinkmeyer, R.; Yeager, C. M.; Santschi, P. H. *Environ. Sci. Technol.* **2010**, *44*, 9042−9048.
(36) Shin, H.-S.; Oh-Shin, Y.-S.; Kim, J.-H.; Ryu, J.-K. *J. Chromatogr. A* **1996**, *732*, 327−333.
(37) Zhang, S.; Du, J.; Xu, C.; Schwehr, K. A.; Ho, Y.-F.; Li, H.-P.; Roberts, K. A.; Kaplan, D. I.; Brinkmeyer, R.; Yeager, C. M.; Chang, H.-S.; Santschi, P. H. *Environ. Sci. Technol.* **2011**, *45*, 5543−5549.
(38) Romarís-Hortas, V.; Bermejo-Barrera, P.; Moreda-Piñeiro, A. *J. Chromatogr. A* **2012**, *1236*, 164−176.
(39) Gómez-Ordóñez, E.; Alonso, E.; Rupérez, P. *Talanta* **2010**, *82*, 1313−1317.
(40) Shah, M.; Wuilloud, R. G.; Kannamkumarath, S. S.; Caruso, J. A. *J. Anal. At. Spectrom.* **2005**, *20*, 176−182.
(41) Pena-Pereira, F.; Senra-Ferreiro, S.; Lavilla, I.; Bendicho, C. *Talanta* **2010**, *81*, 625−629.
(42) Xie, Z.; Zhao, J. *Talanta* **2004**, *63*, 339−343.
(43) Pena-Pereira, F.; Lavilla, I.; Bendicho, C. *Anal. Chim. Acta* **2009**, *631*, 223−228.
(44) Ma, B.; Zeng, F.; Zheng, F.; Wu, S. *Chem.—Eur. J.* **2011**, *17*, 14844−14850.
(45) Singh, N.; Jang, D. O. *Org. Lett.* **2007**, *9*, 1991−1994.
(46) Wu, X.; Chen, J.; Zhao, J. X. *Analyst* **2013**, *138*, 5281−5287.
(47) Qu, F.; Li, N. B.; Luo, H. Q. *Anal. Chem.* **2012**, *84*, 10373−10379.
(48) Wang, Y.; Zhu, H.; Yang, X.; Dou, Y.; Liu, Z. *Analyst* **2013**, *138*, 2085−2089.
(49) Wang, M.; Wu, Z.; Yang, J.; Wang, G.; Wang, H.; Cai, W. *Nanoscale* **2012**, *4*, 4087−4090.
(50) Zhang, J.; Xu, X.; Yang, C.; Yang, F.; Yang, X. *Anal. Chem.* **2011**, *83*, 3911−3917.
(51) Zhang, J.; Yuan, Y.; Xu, X.; Wang, X.; Yang, X. *ACS Appl. Mater. Interfaces* **2011**, *3*, 4092−4100.
(52) Zhang, J.; Xu, X.; Yuan, Y.; Yang, C.; Yang, X. *ACS Appl. Mater. Interfaces* **2011**, *3*, 2928−2931.
(53) Chen, L.; Lu, W.; Wang, X.; Chen, L. *Sens. Actuators, B* **2013**, *182*, 482−488.
(54) Zhou, G.; Zhao, C.; Pan, C.; Li, F. *Anal. Methods* **2013**, *5*, 2188−2192.
(55) Deng, H.-H.; Li, G.-W.; Lin, X.-H.; Liu, A.-L.; Chen, W.; Xia, X.-H. *Analyst* **2013**, *138*, 6677−6682.
(56) Qin, X.; Wang, H.; Miao, Z.; Wang, X.; Fang, Y.; Chen, Q.; Shao, X. *Talanta* **2011**, *84*, 673−678.
(57) Papageorgiou, N.; Maier, W. F.; Grätzel, M. *J. Electrochem. Soc.* **1997**, *144*, 876−884.
(58) Ibupoto, Z. H.; Khun, K.; Willander, M. *Sensors* **2013**, *13*, 1984−1997.
(59) Li, Y.-J.; Tseng, Y.-T.; Unnikrishnan, B.; Huang, C.-C. *ACS Appl. Mater. Interfaces* **2013**, *5*, 9161−9166.
(60) Chen, S.-J.; Huang, C.-C.; Chang, H.-T. *Talanta* **2010**, *81*, 493−498.
(61) Catalano, V. J.; Moore, A. L. *Inorg. Chem.* **2005**, *44*, 6558−6566.
(62) Schmidbaur, H. *Gold Bull.* **2000**, *33*, 3−10.
(63) Schmidbaur, H.; Cronje, S.; Djordjevic, B.; Schuster, O. *Chem. Phys.* **2005**, *311*, 151−161.
(64) Tsipis, C. A.; Karagiannis, E. E.; Kladou, P. F.; Tsipis, A. C. *J. Am. Chem. Soc.* **2004**, *126*, 12916−12929.
(65) Zhu, Y.; Day, C. S.; Zhang, L.; Hauser, K. J.; Jones, A. C. *Chem.—Eur. J.* **2013**, *19*, 12264−12271.
(66) Lasanta, T.; Olmos, M. E.; Laguna, A.; López-de-Luzuriaga, J. M.; Naumov, P. *J. Am. Chem. Soc.* **2011**, *133*, 16358−16361.
(67) Wu, Z. *Angew. Chem., Int. Ed.* **2012**, *51*, 2934−2938.
(68) Ellis, S.; Senanayake, G. *Hydrometallurgy* **2004**, *72*, 39−50.
(69) Jeffrey, M. I.; Ritchie, I. M. *J. Electrochem. Soc.* **2000**, *147*, 3257−3262.
(70) Esmkhani, R.; Ghobadi, B.; Amirkhani, A.; Rezadust, S. *Aust. J. Basic Appl. Sci.* **2013**, *7*, 702−708.
(71) Clark, R. W.; Bonicamp, J. M. *J. Chem. Educ.* **1998**, *75*, 1182−1185.
(72) Michałowski, T.; Asuero, A. G.; Ponikvar-Svet, M.; Toporek, M.; Pietrzyk, A.; Rymanowski, M. *J. Solution Chem.* **2012**, *41*, 1224−1239.
(73) Senanayake, G. *Miner. Eng.* **2004**, *17*, 785−801.
(74) Bryce, R. A.; Charnock, J. M.; Pattrick, R. A. D.; Lennie, A. R. *J. Phys. Chem. A* **2003**, *107*, 2516−2523.
(75) Liu, H.-M.; Xiong, X.-G.; Zhao, C.-C.; Zheng, J.-H.; Gao, Q.-Y. *Acta. Phys.-Chim. Sin.* **2008**, *24*, 1897−1901.
(76) Lu, Y.; Gao, Q.; Xu, L.; Zhao, Y.; Epstein, I. R. *Inorg. Chem.* **2010**, *49*, 6026−6034.